A Hybrid Systems and Optimization-Based Control Approach to Realizing Multi-Contact Locomotion on Transfemoral Prostheses

Huihua Zhao[1], Jonathan Horn[2], Jacob Reher[1], Victor Paredes[2] and Aaron D. Ames[3]

Abstract— **This paper presents a systematic methodology utilizing multi-domain hybrid system models and optimization based controllers to achieve human-like multi-contact prosthetic walking experimentally on a custom-built prosthesis: AMPRO. Inspired by previous work that realized multi-contact locomotion on a bipedal robot AMBER2, a hybrid system based optimization problem is proposed leveraging the framework of multi-domain hybrid systems. Utilizing a reference human gait coupled with physical constraints, the end result of this optimization problem is stable multi-contact prosthetic gaits that can be implemented on the prostheses directly. Leveraging control methods that stabilize bipedal walking robots—control Lyapunov function based quadratic programs coupled with variable impedance control—an online optimization-based controller is formulated to realize the designed gait in both simulation and experimentally on AMPRO. Improved tracking and energy efficiency are seen when this methodology is implemented experimentally. Additionally, the resulting multi-contact prosthetic walking captures the essentials of natural human walking both kinematically and kinetically.**

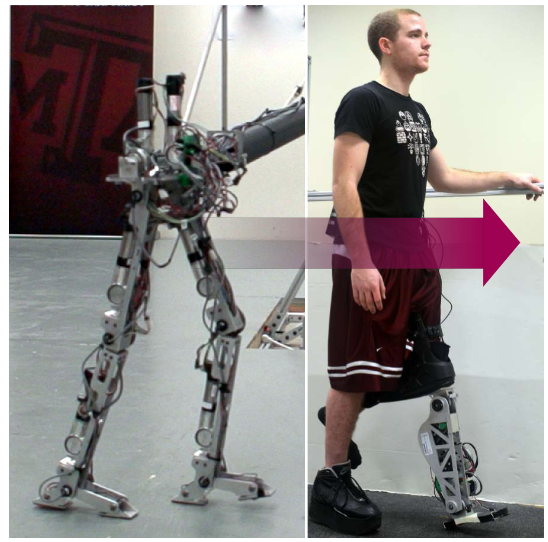

Fig. 1: Multi-contact locomotion capable bipedal robot AMBER2 (left) and healthy human subject with the prosthesis AMPRO in a multi-contact posture (right).

I. INTRODUCTION

Due to the large number of lower-limb amputees needing powered robotic assistive devices [10], there is an increasing demand for more efficient and naturally moving devices. Multi-contact foot behaviors, which are naturally exhibited in human walking [3], [23], are crucial to achieving these goals [14], [17]. This requires the modeling of these behaviors—which is complex due to the changing contact points—and control that guarantees stability and efficiency. As a means to address this need, and the challenges in achieving these behaviors, this paper considers both the modeling of multi-contact locomotion, as it relates to prostheses, and correspondingly constructs controllers for these multi-domain hybrid systems. These contributions are realized experimentally on a novel prosthesis: AMPRO.

Motivated by the advantages and challenges of multi-contact locomotion with foot motion, it has been studied actively in the control and robotic field in the recent decade with the broader goal of achieving close human-like locomotion. In this setting, methods utilizing the popular Zero Moment Point, including gait pattern generation and gait planning methods, are adopted to design the foot trajectory specifically for multi-contact foot behavior in [7], [11], [12]. However, the resulting gait only has foot roll during the double support phase, i.e., the foot remains flat during the stance phase. Simulated robotic walking with significant toe push can be found in [9], [24], in which the authors show that the walking gait with toe push helps reduce torque and achieve faster walking speeds. Different from the above approaches, previous work by the authors [29] started with a hybrid system model motivated by human locomotion, and proposed a novel multi-domain optimization problem which embeds this multi-contact feature into gait design to generate human-like locomotion in a manner that is both formally correct as well as physically realizable. This was combined with a trajectory reconstruction method, with the end result being successful experimental realization of stable human-like multi-contact locomotion on a 7-link 2D bipedal robot AMBER2 as seen in Fig. 1 (see video at [1]).

The main goal of this paper is to extend the framework for achieving multi-contact robotic walking [29], as motivated by previous work by the authors in translating simpler locomotion behaviors to prosthesis [31], to achieve natural prosthetic walking. More explicitly, through utilizing an opt-

*NSF CAREER Award CNS-0953823. This research has approval from the Institutional Review Board with IRB2014-0382F for testing with human.

[1]H. Zhao and J. Reher are with Mechanical Engineering, Georgia Institute of Technology, Atlanta, USA. {huihua, jpreher}@gatech.edu

[2]J. Horn and V. Paredes are with Mechanical Engineering, TAMU, College Station, USA. {j.horn, vcparedesc}@tamu.edu

[3]Prof. A. Ames is with department of Mechanical Engineering and Electrical Engineering, Georgia Institute of Technology, Atlanta, USA. ames@gatech.edu

imal prosthetic gait that is generated based on the hybrid system model of multi-domain locomotion, the main contribution of this paper is the development of an optimization-based controller and its realization of multi-contact prosthetic walking on the custom-built prosthesis: AMPRO. This contribution is accomplished through two novel steps.

The first step is to generate an optimal multi-contact prosthetic gait utilizing a multi-domain hybrid system model. The traditional approach, variable impedance control is a common framework for lower-limb prostheses [8], [22]; by dividing a single step into several phases, a multi-contact prosthetic gait (with heel strike and toe push) can be designed explicitly by carefully choosing control parameters for each phase. A shortcoming of this methodology is that clinicians choose these parameters by trial and error for each individual or each gait, which can be costly and time consuming [4]. This work takes a different approach by constructing a multi-domain hybrid system model for a "robot" with anthropomorphic parameters. Utilizing a low-cost motion capture system for healthy reference human locomotion data collection, a multi-domain optimization problem subject to specific constraints is then proposed to generate a customized stable multi-contact prosthetic gait. The end result is an automatically generated prosthetic gait, which is both optimal and directly implementable for the prosthetic device, therefore, essentially eliminating the requirement of parameter tuning.

Utilizing control methods that stabilize bipedal walking robots, in particular control Lyapunov functions [6], the second step is to formulate a quadratic program based controller that achieves rapidly exponential convergence of virtual constraints subject to actuator bounds. When coupled with impedance control as a feed-forward term, the end result is a model independent quadratic programming (MIQP) controller that is able to achieve better tracking and improved energy efficiency on prostheses. The resulting real-time optimization based controller was experimentally realized on the custom-built prosthesis AMPRO with the end result being multi-contact prosthesis locomotion.

II. Multi-Contact Prosthetic Gait Generation

This section reviews the multi-contact behavior embedded in human locomotion. A motion capture system with inertial measurement units (IMUs) is used to capture the human locomotion data. With the goal of designing a prosthetic gait utilizing robot models, a multi-domain bipedal hybrid system is constructed for a "robot" with anthropomorphic parameters. Based on this model and the reference human locomotion data obtained with the IMUs, a human-inspired optimization problem is constructed for the hybrid system model of multi-contact locomotion [29]; the end result is a customized prosthetic gait that (a) yields theoretically provable stability, (b) captures the essential multi-contact behaviors of healthy human walking and (c) suits the specific test subject wearing the prosthetic device.

A. Multi-Contact Human Locomotion

We begin our analysis of the walking pattern of a normal leg by breaking a single step cycle into different distinct

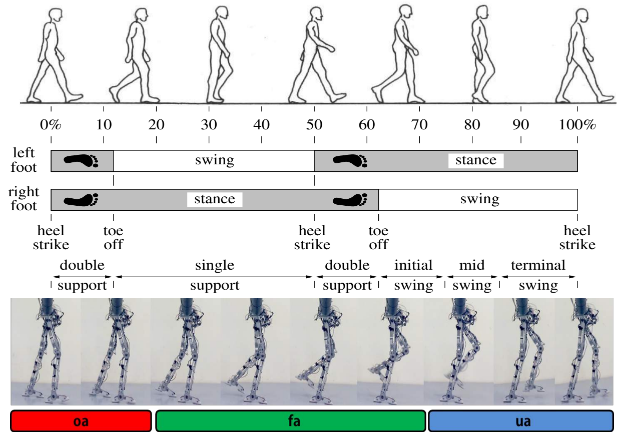

Fig. 2: Multi-contact locomotion diagram of a typical human gait cycle [3] (top) and multi-contact domain break of the bipedal robot AMBER2 (bottom).

phases based on the points of the feet that are in contact with the ground. Utilizing the domain breakdown method discussed in [30], three domains (i.e., sub-phases) of a single step are considered as motivated by the multi-contact walking achieved on the bipedal robot AMBER2 [29]. Based on the actuation type and contact points, we denote the three domains as over-actuated domain, oa (with the stance heel and swing toe in contact with the ground), fully-actuated domain, fa (with the stance heel and toe in the ground) and under-actuated domain, ua (with only stance toe in the ground) as shown in Fig. 2. The switching between domains is triggered by the change of contact points on the feet.

With the goal of obtaining a specific reference gait (i.e., the gait from a healthy subject who has similar anthropomorphic parameters as the amputee), a low-cost inertial motion capture system with IMUs is developed to collect the healthy human planar locomotion data. A model based Extended Kalman Filter (EKF) [21] is used to obtain accurate joint angle information about the human subject [31]. During the experiments, the subject was asked to walk along a straight line in a normal self-selected cadence for several steps, the data of which are averaged to yield the unique reference trajectories for the optimization problem that will be discussed later.

B. Multi-Contact Robot Model

Considering the changes of foot contact points over a gait cycle (lifting and striking of the heel and toe), a hybrid system model is developed, i.e., a model with both continuous and discrete dynamics. Formally, a multi-domain walking gait can be modeled as a hybrid control system [25] given by the following tuple:

$$\mathscr{HC} = (\Gamma, D, U, S, \Delta, FG), \tag{1}$$

where

- $\Gamma = (V, E)$ is a *directed cycle*, with vertices $V = \{\text{oa}, \text{fa}, \text{ua}\}$; and edges $E = \{e_1 = \{\text{oa} \to \text{fa}\}, e_2 = \{\text{fa} \to \text{ua}\}, e_3 = \{\text{ua} \to \text{oa}\}\}$,

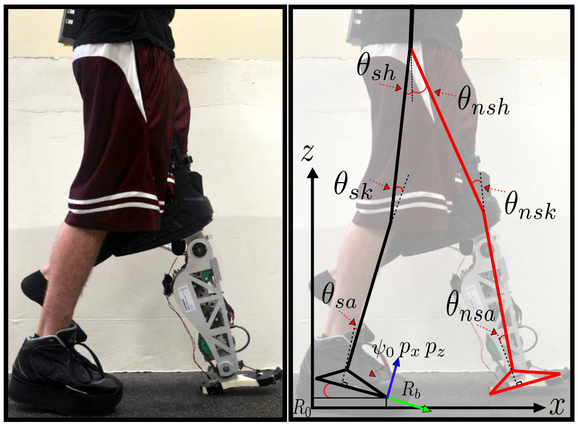

Fig. 3: Subject with the prosthesis AMPRO (left) and multi-contact configuration of the robotic model (right).

- $D = \{D_{\text{oa}}, D_{\text{fa}}, D_{\text{ua}}\}$, set of *domains of admissibility*,
- $U = \{U_{\text{oa}}, U_{\text{fa}}, U_{\text{ua}}\}$, set of *admissible controls*,
- $S = \{S_{\text{oa}\to\text{fa}}, S_{\text{fa}\to\text{ua}}, S_{\text{ua}\to\text{oa}}\}$, set of *guards*,
- $\Delta = \{\Delta_{\text{oa}\to\text{fa}}, \Delta_{\text{fa}\to\text{ua}}, \Delta_{\text{ua}\to\text{oa}}\}$, set of *reset maps*,
- $FG = \{(f_v, g_v)\}_{v\in V}$ with (f_v, g_v) a *control system* on D_v, i.e., $\dot{x} = f_v(x) + g_v(x)u_v$ for $x \in D_v$ and $u_v \in U$.

The detailed explanation of each element of this hybrid system is omitted here and can be found in [16], [29].

The configuration space Q of the robot is characterized by the generalized coordinates: $\theta = \{p_x, p_z, \varphi_0, \theta_b\}$, where the extended coordinates $\{p_x, p_z, \varphi_0\}$ represent the position and rotation angle of the body fixed frame R_b with respect to the world frame R_0; and $\theta_b = \{\theta_{sa}, \theta_{sk}, \theta_{sh}, \theta_{nsh}, \theta_{nsk}, \theta_{nsa}\}$ denotes the body coordinates shown in Fig. 3. The dynamics on each domain can be obtained from general "unpinned" model through the use of holonomic constraints [18], [26]:

$$\begin{aligned} M(\theta)\ddot{\theta} + H(\theta,\dot{\theta}) &= B(\theta)u + J_v(\theta)^T F_v(\theta,\dot{\theta},u), \\ J_v(\theta)\ddot{\theta} + \dot{J}_v(\theta)\dot{\theta} &= \mathbf{0}, \end{aligned} \tag{2}$$

where $M(\theta) \in \mathbb{R}^{9\times 9}$ is the inertial matrix, and $H(\theta,\dot{\theta}) \in \mathbb{R}^{9\times 1}$ contains the terms resulting from the Coriolis effect $C(\theta,\dot{\theta})\dot{\theta}$ and the gravity vector $G(\theta)$. $B(\theta)$ denotes the torque distribution matrix. $J_v(\theta)$ is the Jacobian of specific contact points of the corresponding domain $v \in V$. $F_v(\theta,\dot{\theta})$ are the reaction forces due to the holonomic constraints and defined specifically based on the contact conditions of the heel and toe [18]. With the notation $x = (\theta;\dot{\theta})$, the affine control system $\dot{x} = f_v(x) + g_v(x)u$ for each domain D_v with $v \in V$ can be obtained by reformulating (2) [20]. The discrete behavior of impacts (including toe strike and heel strike of the multi-contact model) is modeled with the perfectly plastic impact assumption; more details can be found in [13], [29].

C. Human-Inspired Outputs

We begin by viewing the complex human locomotion system as a "black box." Therefore, the goal of achieving human-like robotic walking becomes to drive the actual robot outputs $y^a(\theta)$ to the desired human outputs $y^d(t,\alpha)$ that are represented by a specific walking function (see [29]). In particular, a total of 7 outputs are of interest for the multi-domain 7-link bipedal robot, which yields the human-inspired outputs [5]:

$$y(\theta,\dot{\theta},\alpha) = \begin{bmatrix} y_1(\theta,\dot{\theta},\alpha) \\ y_2(\theta,\alpha) \end{bmatrix} = \begin{bmatrix} y_1^a(\theta,\dot{\theta}) - v_{hip} \\ y_2^a(\theta) - y_2^d(\rho(\theta),\alpha) \end{bmatrix}, \tag{3}$$

where $y_1(\theta,\dot{\theta},\alpha)$ and $y_2(\theta,\alpha)$ are the relative degree one output and relative degree two outputs, respectively. The parameter set α is the grouped parameters of all the outputs consisting of both the relative degree one output and relative degree two outputs for a complete step cycle [29]. Based on the actuation type in each domain D_v with $v \in V$, the corresponding components α_v of α will be utilized to define the human-inspired outputs. Importantly, for a specific output, the parameters will be kept unchanged for all the domains.

Upon observation of multi-contact human locomotion data, the linearized forward hip position, $\delta p_{hip}(\theta)$, was discovered to increase linearly through the progress of a step [15]; this motives the following phase variable:

$$\rho(\theta) = (\delta p_{hip}(\theta) - \delta p_{hip}^{+})/v_{hip}, \tag{4}$$

aiming to remove the dependency of time [5], [26]; here $\delta p_{hip}^{+}(\theta)$ is the hip position at the beginning of a step.

Partial Hybrid Zero Dynamics. The human-inspired controller as discussed in [5] can be utilized to drive both $y_1 \to 0$ and $y_2 \to 0$ in a provably exponentially stable fashion for the continuous dynamics. However, the robot will "bounce-off" the designed trajectory when impacts occur. This motivates the introduction of the *partial hybrid zero dynamics* (PHZD) constraints aiming to produce a parameter set α that ensures the tracking of relative degree two outputs remain invariant through impacts. In particular, with the *partial zero dynamics* (PZD) surface defined as:

$$\mathbf{PZ}_\alpha = \{(\theta,\dot{\theta}) \in Q : y_2(\theta,\alpha) = \mathbf{0}, L_f y_2(\theta,\alpha) = \mathbf{0}\}, \tag{5}$$

the general PHZD constraints can be stated abstractly as:

$$\Delta(S \cap \mathbf{PZ}_\alpha) \subseteq \mathbf{PZ}_\alpha, \tag{PHZD}$$

which are required to be valid through all three discrete transitions as illustrated in (1). Explicitly, the three sets of PHZD constraints can be stated as:

$$\Delta_{oa\to fa}(S_{oa\to fa} \cap \mathbf{PZ}_{\alpha_{oa}}) \subseteq \mathbf{PZ}_{\alpha_{fa}}, \tag{PHZD1}$$

$$\Delta_{fa\to ua}(S_{fa\to ua} \cap \mathbf{PZ}_{\alpha_{fa}}) \subseteq \mathbf{PZ}_{\alpha_{ua}}, \tag{PHZD2}$$

$$\Delta_{ua\to oa}(S_{ua\to oa} \cap \mathbf{PZ}_{\alpha_{ua}}) \subseteq \mathbf{PZ}_{\alpha_{oa}}. \tag{PHZD3}$$

The detailed construction of these constraints requires the explicit explanation of techniques such as the reduced order hybrid zero dynamics, inverse kinematics and PHZD reconstructions, which are omitted here for simplicity of the paper structure. The details can be found in [16], [29].

D. Multi-Contact Prosthetic Gait Design

By enforcing the PHZD constraints discussed above, a multi-contact human-inspired optimization is utilized to design walking trajectories that are both provably stable and human-like [5], [29]. More importantly, physical constraints

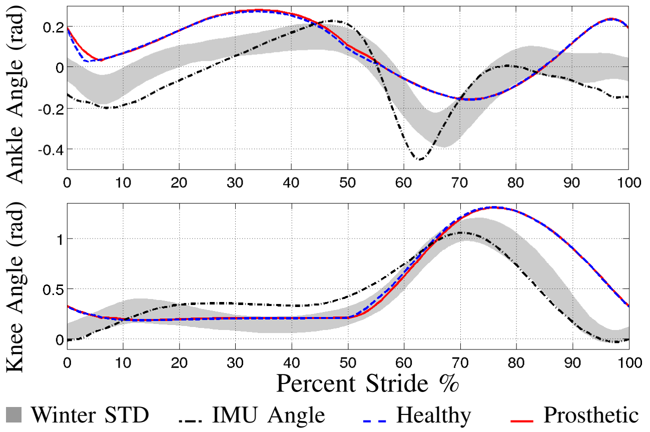

Fig. 4: Joint angles for human subject collected with IMUs and the simulated healthy walking and prosthetic walking as compared to Winter data [27].

of the prosthetic device with the consideration of (a) hardware limits (torque limits and joint movement range), (b) safety concern (torque optimality and velocity limits) and (c) user comfortability (user preferred trajectory profile) are considered during the gait design [31]. These specifications yield the multi-contact optimization problem subject to both PHZD and physical constraints:

$$\begin{aligned} \alpha^* = \underset{\alpha\in\mathbb{R}^{43}}{\text{argmin}}\ & \text{Cost}_{\text{HD}}(\alpha) \\ \text{s.t}\ \ & (\text{PHZD1})-(\text{PHZD3}), \\ & \text{Physical Constraints}, \end{aligned} \tag{6}$$

where the cost function is the least-square-fit error between the reference human data and the chosen walking function representations [5]. The immediate result of this optimization problem is the output parameter set α that renders a provably stable and optimal (w.r.t. torque, foot clearance, joint position and velocity) multi-contact prosthetic gait, which can be implemented directly on the prosthetic device. The desired joint angles and angular velocities for the prosthetic device can be obtained through the inverse projection from the PHZD surface by only knowing the actual forward hip position (see (4)) and the corresponding hip velocity [5], [29]. The desired trajectories of both the ankle and knee, as shown in Fig. 4, are obtained and compared with the human locomotion data obtained from both the IMU collection system and Winter [27]. Both the knee and ankle angles are shown to have a similar pattern as the nominal data.

III. PROSTHETIC CONTROLLER DESIGN

This section begins by briefly introducing a real-time optimization-based prostheses controller, which has been proposed in [28] and validated in [31] for achieving flat-foot prosthetic walking on a custom built prosthesis, AMRPO. With the multi-contact trajectories in hand, the controller is then implemented to achieve prosthetic walking in simulation at the end of this section.

A. MIQP+Impedance Control

In previous work [31], the authors proposed a novel prosthetic controller that combines the *rapidly exponentially stabilizing control Lyapunov functions* (RES-CLFs) based quadratic program control [6] with impedance control in an effort to achieve better tracking and improved energy efficiency on prostheses. In particular, using the human-inspired feedback linearization controller [5], equation (2) can be converted to a linear form as follows:

$$\dot{\eta} = \underbrace{\begin{bmatrix} 0_{2\times2} & I_{2\times2} \\ 0_{2\times2} & 0_{2\times2} \end{bmatrix}}_{F} \eta + \underbrace{\begin{bmatrix} 0_{2\times2} \\ I_{2\times2} \end{bmatrix}}_{G} \mu, \tag{7}$$

where $\eta = (y_p; \dot{y}_p) \in \mathbb{R}^{4\times1}$ with $y_p = (\theta_a^p, \theta_k^p)^T$ the angles for the prosthetic ankle joint and knee joint, respectively. Leveraging the Continuous Algebraic Riccati Equations with solution $P = P^T > 0$, allows for the construction of a RES-CLF [6] given as:

$$V_\varepsilon(\eta) = \eta^T \begin{bmatrix} \frac{1}{\varepsilon} I & 0 \\ 0 & I \end{bmatrix} P \begin{bmatrix} \frac{1}{\varepsilon} I & 0 \\ 0 & I \end{bmatrix} \eta := \eta^T P_\varepsilon \eta, \tag{8}$$

with the convergence rate $\varepsilon > 0$. In order to exponentially stabilize the system, we want to find μ such that, for a chosen $\gamma > 0$ [6], we have:

$$L_F V_\varepsilon(\eta) + L_G V_\varepsilon(\eta)\mu \le -\frac{\gamma}{\varepsilon} V_\varepsilon(\eta), \tag{9}$$

where $L_F V_\varepsilon(\eta)$ and $L_G V_\varepsilon(\eta)$ are the corresponding Lie derivatives of the Lyapunov function (8) relative to (7). Particularly, an optimal (point-wise) μ could be found by turning this condition into a quadratic problem (QP) while enforcing a relaxation term $\delta > 0$ for torque optimality. More importantly, we add the variable impedance term μ^{imp} into the construction for the total hardware torque bounds, which yields the following model independent quadratic program plus impedance control (MIQP+Impedance):

$$\begin{aligned} \underset{(\delta,\mu^{qp})\in\mathbb{R}^{2+1}}{\text{argmin}}\ & p\delta^2 + \mu^{qp^T}\mu^{qp} & (10) \\ \text{s.t}\ \ & L_F V_\varepsilon(\eta) + \frac{\gamma}{\varepsilon} V_\varepsilon(\eta) + L_G V_\varepsilon(\eta)\mu^{qp} \le \delta, & \text{(CLF)} \\ & \mu^{qp} \le \mu^{qp}_{MAX}, & \text{(Max QP Torque)} \\ & -\mu^{qp} \le \mu^{qp}_{MAX}, & \text{(Min QP Torque)} \\ & \mu^{qp} \le \mu_{MAX} - \mu^{imp}, & \text{(Max Input Torque)} \\ & -\mu^{qp} \le \mu_{MAX} + \mu^{imp}, & \text{(Min Input Torque)} \end{aligned}$$

This QP problem yields an optimal controller that regulates the output errors in a rapidly exponentially stable fashion. Additionally, the model independent controller gathers information about the system through the addition of the feed-forward impedance control to the input torque. By setting the QP torque bounds μ^{qp}_{MAX}, we can limit the overshoot problems. We also set the total input torque bounds for the QP problem such that the final optimal input torque will satisfy the hardware torque bounds μ_{MAX}, which is critical for practical implementation.

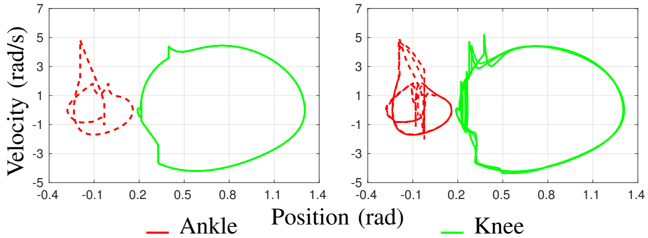

(a) Healthy Walking (b) Prosthetic Walking

Fig. 5: Phase portraits of prosthesis joints for the simulated healthy walking and prosthetic walking.

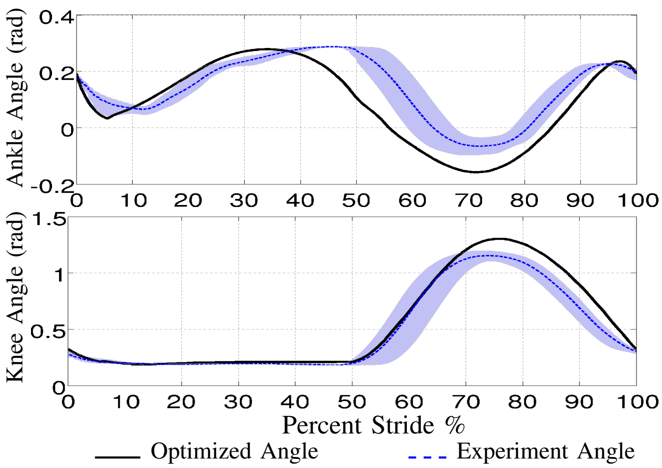

Fig. 6: Averaged experimental joint angles compared with the designed joint angles obtained from optimization. Grey area is the one standard deviation of the experiment results.

B. Simulation Results

Considering the complexity of multi-contact locomotion (multiple impacts and switching between different actuation types of domains), the control architecture is first verified in simulation. The limit cycles of both the healthy human walking and the prosthetic walking (using MIQP+Impedance control for the prosthetic joints) are shown in Fig. 5. The stability of both the multi-contact gaits was numerically validated through the Poincaré map [19], wherein the magnitude of the maximum eigenvalue was found to be $5.5e^{-8}$ using human-inspired control and $5.5e^{-4}$ using MIQP+Impedance control, therefore, indicating the stability of both controllers.

IV. EXPERIMENTAL REALIZATION

Utilizing the optimal multi-contact gait generated in Sec. II and the control architecture introduced in Sec. III, we now have the framework to realize the main contribution of this paper experimentally on a custom-built prosthesis AMPRO to achieve dynamic multi-contact walking. The resulting walking using the real-time optimization-based controller will be compared with other controllers.

A. AMPRO and IMU sensing

AMPRO (**AM**BER **Pro**sthetic) is a custom designed self-contained transfemoral prosthetic device, which includes two brushless DC motors to actuate both the ankle and knee joints in the sagittal plane. Two FlexiForce force sensors are mounted at the toe and heel to detect foot contact, which will be used for stance-swing switching. More details about the design specifications can be found in [31]. To provide a point of human-robotic interaction, two IMUs are mounted on the shin and thigh of the human leg for measuring relative orientation and velocity for both the knee and ankle. In particular, while the human leg is in stance, IMU readings are utilized to compute the forward hip position and forward hip velocity; therefore, the desired swing trajectories of the prosthetic can be calculated accordingly using the PHZD reconstruction method discussed in Sec. II.

B. Experiment Results

A PD controller μ^{pd} is first implemented to track the designed trajectories to achieve stable walking. Walking trials were performed on a treadmill providing a constant speed of 1.3 mph. The impedance parameters are estimated based on the experimental walking data obtained using the PD controller. The detailed estimation method can be referred to [31]. We then apply impedance control μ^{imp} as the feed-forward term while using the MIQP control μ^{qp} as the feed-back term to track the desired joint trajectories. The resulting joint trajectories are shown in Fig. 6, and the experimental gait tiles along with the simulated prosthetic walking are shown in Fig. 7. A video of the resulting multi-contact walking can be seen at [2]. Therefore, utilizing the systematic methodology including gait design and optimization-based control, AMPRO successfully achieved stable and human-like multi-contact walking.

In particular, with the goal of showing the torque optimality of the proposed controller, different torque bounds (high torque 100 Nm for MIQPH and low torque 40 Nm MIQPL) for both μ_{MAX} and μ^{qp}_{MAX} are tested during the experiment. We also compare it with an augmented control strategy, PD+Impedance (i.e., $\mu^d = \mu^{pd} + \mu^{imp}$), which also includes impedance control as a feed-forward term. The comparing results (including *rms* errors and power consumption) of using different controllers are shown in Fig. 8. From this figure, we can see that the tracking performances of both the ankle and knee are the best with MIQPH+Imp control. Importantly, the better performance doesn't require more energy when compared with PD+Impedance control. Similar results can also be found when comparing MIQPL+Impedance and PD control. To summarize, we can conclude that the MIQP+Impedance controller has the best balanced performance between tracking and power requirements.

V. CONCLUSIONS

By leveraging a systematic methodology—including hybrid system models and real-time optimization-based controllers—this paper successfully translated the multi-contact behavior that is intrinsic in human locomotion from bipedal walking on AMBER2 to prosthetic walking on the prosthesis AMPRO. The performance of multiple controllers—utilized to track the generated optimal multi-contact gait—are compared with the real-time optimization

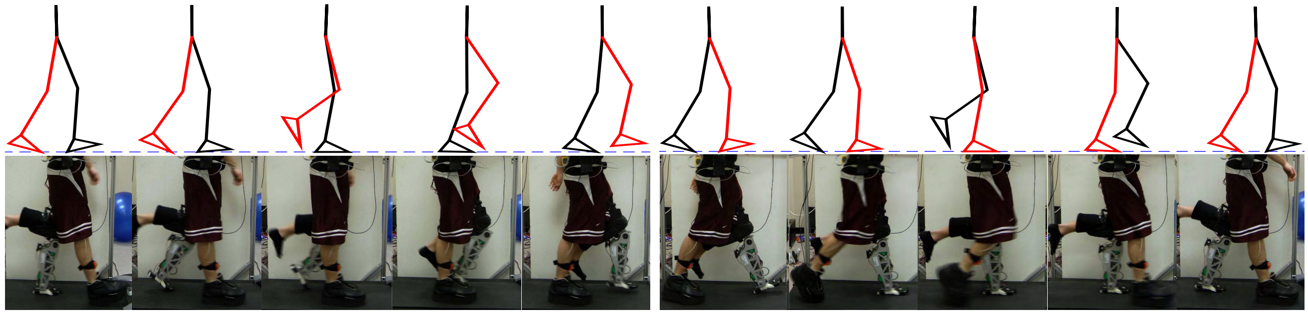

Fig. 7: Gait tile comparisons between the simulated and the experimental prosthetic walking using MIQP+Imp control.

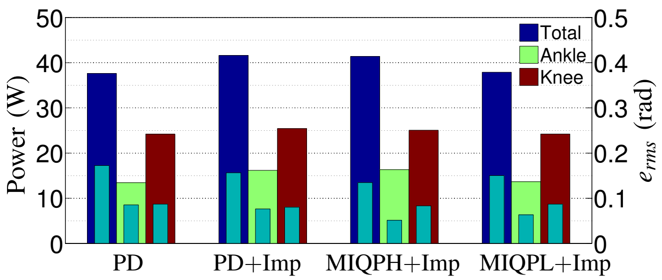

Fig. 8: Net power (thick bar) and *rms* tracking error (thin bar) comparisons of the prosthetic joints of one step (including stance phase and swing phase) with using different control methods as averaged over 10 steps.

based controller resulting in the best overall performance. The obtained prosthetic walking is shown to capture the essentials of human walking both kinematically and kinetically, resulting in a smoother and more comfortable user experience when compared to flat-footed walking.

References

[1] Multi-Contact Robotic Walking of AMBER. https://youtu.be/VvkIdCKlL54.

[2] Realization of Multi-Contact Prosthetic Walking with AMPRO. https://youtu.be/K6mKYrVYVwE.

[3] M. Ackermann. *Dynamics and Energetics of Walking with Prostheses*. PhD thesis, University of Stuttgart, Stuttgart, March 2007.

[4] N. Aghasadeghi, H. Zhao, L. J. Hargrove, A. D. Ames, E. J. Perreault, and T. Bretl. Learning impedance controller parameters for lower-limb prostheses. In *Intelligent Robots and Systems, IEEE International Conference on*, pages 4268 – 4274, 2013.

[5] A. D. Ames. Human-inspired control of bipedal walking robots. *Automatic Control, IEEE Transactions on*, 59(5):1115–1130, 2014.

[6] A. D. Ames, K. Galloway, K. Sreenath, and J. W. Grizzle. Rapidly exponentially stabilizing control lyapunov functions and hybrid zero dynamics. *Automatic Control, IEEE Transactions on*, 59(4):876–891, 2014.

[7] G. Bessonnet, P. Seguin, and P. Sardain. A parametric optimization approach to walking pattern synthesis. *International Journal Robotic Research*, 24(7):523–536, Jul 2005.

[8] A. Blank, A. M. Okamura, and L. L. Whitcomb. User comprehension of task performance with varying impedance in a virtual prosthetic arm: A pilot study. In *Biomedical Robotics and Biomechatronics, 4th EMBS International Conference on*, pages 500–507, 2012.

[9] C. Chevallereau, D. Djoudi, and J. W. Grizzle. Stable bipedal walking with foot rotation through direct regulation of the zero moment point. *Robotics, IEEE Transactions on*, 24(2):390–401, April 2008.

[10] T. Dillingham. Limb amputation and limb deficiency: Epidemiology and recent trends in the united states. *Southern Medical Journal*, 2002.

[11] N. Handharu, J. Yoon, and G. Kim. Gait pattern generation with knee stretch motion for biped robot using toe and heel joints. In *Humanoid Robots, 8th International Conference on*, pages 265–270. IEEE, 2008.

[12] Q. Huang, K. Yokoi, S. Kajita, K. Kaneko, H. Arai, N. Koyachi, and K. Tanie. Planning walking patterns for a biped robot. *IEEE Transactions on Robotics and Automation*, 17:280–289, 2001.

[13] Y. Hürmüzlü and D. B. Marghitu. Rigid body collions of planar kinematic chains with multiple contact points. *Intl. J. of Robotics Research*, 13(1):82–92, February 1994.

[14] V. T. Inman and J. Hanson. Human locomotion. In *Human Walking*. Williams & Wilkins, Baltimore, 1994.

[15] S. Jiang, S. Partrick, H. Zhao, and A. D. Ames. Outputs of human walking for bipedal robotic controller design. In *American Control Conference (ACC), 2012*, pages 4843–4848, June 2012.

[16] J. Lack, M.J. Powell, and A. D. Ames. Planar multi-contact bipedal walking using hybrid zero dynamics. In *Robotics and Automation (ICRA), 2014 IEEE International Conference on*, pages 2582–2588.

[17] D. C. Morgenroth, A. D. Segal, K. E. Zelik, J. M. Czerniecki, G. K. Klute, P. G. Adamczyk, M. S. Orendurff, M. E. Hahn, S. H. Collins, and A. D. Kuo. The effect of prosthetic foot push-off on mechanical loading associated with knee osteoarthritis in lower extremity amputees. *Gait & posture*, 34(4):502–507, 2011.

[18] R. M. Murray, Z. Li, and S. S. Sastry. *A Mathematical Introduction to Robotic Manipulation*. CRC Press, Boca Raton, March 1994.

[19] T. S. Parker and L. O. Chua. *Practical numerical algorithms for chaotic systems*. Springer Science & Business Media, 2012.

[20] S. S. Sastry. *Nonlinear Systems: Analysis, Stability and Control*. Springer, New York, June 1999.

[21] S. Šlajpah, R. Kamnik, and M. Munih. Kinematics based sensory fusion for wearable motion assessment in human walking. *Computer methods and programs in biomedicine*, 116(2):131144, 2014.

[22] F. Sup, A. Bohara, and M. Goldfarb. Design and Control of a Powered Transfemoral Prosthesis. *The International journal of robotics research*, 27(2):263–273, February 2008.

[23] D. H. Sutherland, K. R. Kaufman, and J. R. Moitoza. *Human Walking*. Williams & Wilkins, Baltimore, 1994.

[24] D. Tlalolini, C. Chevallereau, and Y. Aoustin. Comparison of different gaits with rotation of the feet for a planar biped. *Robotics and Autonomous Systems*, 57(4):371 – 383, 2009.

[25] R. Vasudevan, A. D. Ames, and R. Bajcsy. Using persistent homology to determine a human-data based cost for bipedal walking. In *18th IFAC World Congress*, Milano, Italy, 2011.

[26] E. R. Westervelt, J. W. Grizzle, C. Chevallereau, J. H. Choi, and B. Morris. *Feedback Control of Dynamic Bipedal Robot Locomotion*. CRC Press, Boca Raton, June 2007.

[27] D. A. Winter. *Biomechanics and Motor Control of Human Movement*. Wiley-Interscience, New York, 2 edition, May 1990.

[28] H. Zhao, S. Kolathaya, and A. D. Ames. Quadratic programming and impedance control for transfemoral prosthesis. In *Robotics and Automation, International Conference on*, pages 1341 – 1347, 2014.

[29] H. Zhao, W.-L Ma, M. B. Zeagler, and A. D. Ames. Human-inspired multi-contact locomotion with amber2. In *Cyber-Physical Systems (ICCPS), International Conference on*, pages 199–210, April 2014.

[30] H. Zhao, M. J. Powell, and A. D. Ames. Human-inspired motion primitives and transitions for bipedal robotic locomotion in diverse terrain. *Optimal Control Applications and Methods*, 35(6):730–755, 2014.

[31] H. Zhao, J. Reher, J. Horn, V. Paredes, and A. D. Ames. Realization of nonlinear real-time optimization based controllers on self-contained transfemoral prosthesis. In *Cyber Physics System, 6th International Conference on*, pages 130–138, Seattle, WA, 2015.